

**Magnon dynamics in a skyrmion-textured domain wall of antiferromagnets**Seungho Lee<sup>1</sup>, Kouki Nakata<sup>2</sup>, Oleg Tchernyshyov<sup>3</sup>, and Se Kwon Kim<sup>1</sup><sup>1</sup>*Department of Physics, Korea Advanced Institute of Science and Technology, Daejeon 34141, Republic of Korea*<sup>2</sup>*Advanced Science Research Center, Japan Atomic Energy Agency, Tokai, Ibaraki 319-1195, Japan*<sup>3</sup>*William H. Miller III Department of Physics and Astronomy, Johns Hopkins University, Baltimore, Maryland 21218, USA*

(Received 14 November 2022; revised 17 April 2023; accepted 20 April 2023; published 16 May 2023)

We theoretically investigate the interaction between magnons and a skyrmion-textured domain wall in a two-dimensional antiferromagnet and elucidate the resultant properties of magnon transport. Using supersymmetric quantum mechanics, we solve the scattering problem of magnons on top of the domain wall and obtain the exact solutions of propagating and bound magnon modes. Then, we find their properties of reflection and refraction in the skyrmion-textured domain wall, where magnons experience an emergent magnetic field due to their nontrivial spin texture-induced effective gauge field. Based on the obtained scattering properties of magnons and the domain wall, we show that the thermal transport decreases as the domain wall's chirality increases. Our results suggest that the thermal transport of an antiferromagnet is tunable by modulating the skyrmion charge density of the domain wall, which might be useful for realizing electrically tunable spin caloritronic devices.

DOI: [10.1103/PhysRevB.107.184432](https://doi.org/10.1103/PhysRevB.107.184432)**I. INTRODUCTION**

Antiferromagnets are arising platforms for spintronic applications due to their exceptional features [1,2]. Antiferromagnets have negligible net magnetic moments, which thereby make antiferromagnets robust against external magnetic stimuli. Moreover, the absence of the net magnetic moment allows us to ignore the effects of stray fields which have been hampering the densification of ferromagnetic devices. Compared to ferromagnets whose dynamics are on the gigahertz scale, the inherent dynamics of antiferromagnets are in the range of terahertz that supports the antiferromagnet as a candidate for an ultrafast computation platform [3,4].

Elementary magnetic excitations of an antiferromagnetic system exhibit left- and right-circular spin waves [5–8]. A quantum of the spin wave is a spin-1 boson and is called a magnon [9]. The magnon current can be free from the electron current, which is the classic information carrier of electronics but inevitably implies Ohmic loss. Therefore magnons are considered as promising candidates of information carriers for low-energy-based devices [10]. Not only fundamental interest for excitations of ordered magnetic systems but also potential technological usefulness derives research branches such as magnonics [11] and spin caloritronics [12].

Topological solitons are topologically classified stable solutions of field theory [13–17]. They are found and studied in research areas such as nuclear physics [18,19], soft matter physics [20–26], optics [27,28], and condensed matter physics [29–38]. One of the mostly studied topological solitons is the skyrmion [39,40]. The skyrmion was suggested in the early 1960s and has been considered as a key to describe baryonic matters in nuclear physics [41,42]. The originally suggested skyrmion which resides in the three-dimensional space is defined by the homotopy group  $\pi_3(S^3)$ . A magnetic skyrmion is the two-dimensional (2D) version of the original skyrmion, called the baby skyrmion in the high-energy

community, and defined by  $\pi_2(S^2)$ . In the condensed matter community, magnetic skyrmions are simply called skyrmions. Similarly skyrmions are generalized to  $N$ -dimension space and defined by  $\pi_N(S^N)$  [43]. From now on we use the term “skyrmion” to refer to the magnetic skyrmion.

Two-dimensional antiferromagnets support topological solitons such as skyrmions and domain walls [44–48]. Skyrmions are pointlike localized in two dimensions and domain walls are pointlike localized in one dimension [17,49]. These localities have an advantage in information technology [50–52]. Furthermore, topological solitons can be used as controllers of magnon currents via the interaction of magnons and topological solitons [53]. In particular, a magnon on nontrivial spin textures feels the gauge field so that it experiences the effective Lorentz force which generates the transverse dynamics of the magnon [54–57]. The nontrivial textures frequently become the essence of the transverse transports and also determine the nontrivial properties of the longitudinal transport [58–60].

In this paper, we investigate the interaction of magnons and a skyrmion-textured domain wall, which is a topological soliton having properties of the skyrmion and the domain wall [61,62], in two-dimensional antiferromagnets. The skyrmion-textured domain wall shows a chiral texture along the domain wall represented by the topological charge density and determined by boundary conditions that is illustrated in Fig. 1. Domain walls with no spin texture along with them are known to be transparent to magnons [63,64]. However, the skyrmion-textured domain wall is no longer transparent, since the chiral texture makes a reflective potential barrier for the magnon [62]. To obtain the reflection probability, we use supersymmetric (SUSY) quantum mechanics (QM) [65,66]. We also obtain the exact solutions of magnon-bound modes in the vicinity of the domain wall. Based on the Lagrangian formalism, we derive the gauge field for the magnon and interpret

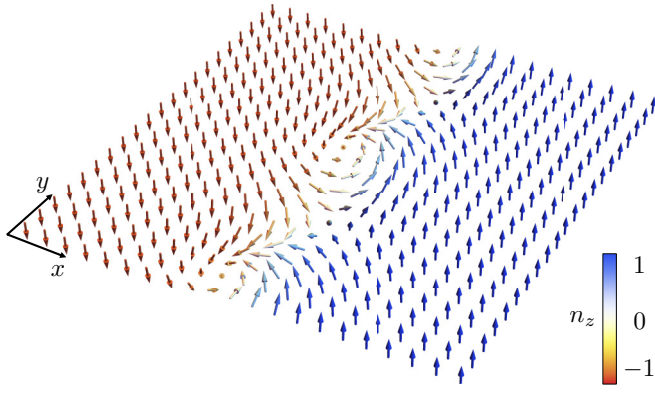


FIG. 1. A skyrmion-textured domain wall. The arrows represent the Néel order parameter  $\mathbf{n}$ . The color represents the  $z$  component of the Néel order parameter.

the magnon refraction as a deflection of the magnon trajectory due to the emergent magnetic field.

Reflection and refraction phenomena affect the thermal transport of the sample, and thus the thermal transport is vividly chirality dependent. Generically, the thermal transport is determined by the material parameters of a given sample which are not easy to tune rapidly. Here using the chiral texture, we propose potentially useful means to tune the thermal transport. To elucidate the tunable thermal transport, we use domain walls in an easy-axis antiferromagnet. The easy-axis anisotropy breaks the spin  $O(3)$  symmetry down to  $U(1)$  and the domain wall spontaneously breaks this  $U(1)$  symmetry. In a two-dimensional system, a domain wall is a one-dimensional object and spin textures can spatially vary along the domain wall when chirality is injected [60,67–71]. The chirality injection is tunable by the spin Hall effect of a metal contact at the boundary of the domain wall. This tunability of the spin chirality manifests the tunable thermal transport.

This paper is organized as follows. We begin in Sec. II by formulating the field theory for two-dimensional antiferromagnets and introduce the skyrmion-textured domain wall. Section III is devoted to understanding the interaction of magnons and the skyrmion-textured domain wall via SUSY QM and the emergent electromagnetism. In Sec. IV, we show the chirality dependence of the thermal transport. In Sec. V, we summarize and conclude our paper. In Appendix A, we derive equations of motion for the antiferromagnet via the Poisson bracket. Appendix B provides detailed calculations of the gauged sigma model [72–74]. From the gauged sigma model approach, we can naturally see how the gauge field of the magnetic order generates the gauge field of the magnetic excitation.

## II. SKYRMION-TEXTURED DOMAIN WALLS IN A 2D ANTIFERROMAGNET

In this section, using the continuum field theory of Lagrange-Hamilton formalism, we formulate a two-dimensional antiferromagnet and introduce the skyrmion-textured domain wall.

### A. General formalism

We consider a two-dimensional collinear antiferromagnet with easy-axis anisotropy, where the magnetizations of two constituent sublattices are antiferromagnetically coupled [75–78]. The state of the antiferromagnet is represented by the Néel order parameter  $\mathbf{n}(\mathbf{x}, t)$  which is a three-dimensional unit vector in the direction of the staggered magnetization, i.e., the difference of the magnetization between the two sublattices. The Lagrangian of the system is a functional of the order parameter  $\mathbf{n}$ , whose density is given by [79–81]

$$\mathcal{L} = \frac{1}{2} \left\{ \rho |\dot{\mathbf{n}}|^2 - A \sum_i |\partial_i \mathbf{n}|^2 - K [1 - (\mathbf{n} \cdot \hat{z})^2] \right\}, \quad (1)$$

where  $\rho$ ,  $A$ , and  $K$  are the inertia of the staggered magnetization, the exchange coefficient, and the anisotropy coefficient, respectively. For the subsequent theoretical discussion, it is convenient to use the natural unit of length, time, and energy by setting  $\rho = A = K = 1$ , in which the Lagrangian density is given by

$$\mathcal{L} = \frac{1}{2} \left\{ |\dot{\mathbf{n}}|^2 - \sum_i |\partial_i \mathbf{n}|^2 - [1 - (\mathbf{n} \cdot \hat{z})^2] \right\}. \quad (2)$$

Since the order parameter  $\mathbf{n}$  has unit length, it can be expressed by two fields  $\theta$  and  $\phi$  by

$$\mathbf{n}(\mathbf{x}, t) = (\sin \theta \cos \phi, \sin \theta \sin \phi, \cos \theta), \quad (3)$$

$$\theta = \theta(\mathbf{x}, t), \quad \phi = \phi(\mathbf{x}, t). \quad (4)$$

Since  $|\dot{\mathbf{n}}|^2 - \sum_i |\partial_i \mathbf{n}|^2 = \partial_\mu \mathbf{n} \cdot \partial^\mu \mathbf{n} = \partial_\mu \theta \partial^\mu \theta + \sin^2 \theta (\partial_\mu \phi \partial^\mu \phi)$  from Eq. (3), we obtain the Lagrangian in terms of two fields  $\theta$  and  $\phi$ :

$$\mathcal{L} = \frac{1}{2} [\partial_\mu \theta \partial^\mu \theta + \sin^2 \theta (\partial_\mu \phi \partial^\mu \phi) - \sin^2 \theta]. \quad (5)$$

Here, we use Einstein's summation convention and the metric signature is  $[+, -, -]$  (2+1 space-time metric). The following coupled equations of motion for the fields  $\theta$  and  $\phi$  are obtained from the Euler-Lagrange equations:

$$\partial_\mu \partial^\mu \theta - \sin \theta \cos \theta (\partial_\mu \phi \partial^\mu \phi - 1) = 0, \quad (6)$$

$$\partial_\mu (\sin^2 \theta \partial^\mu \phi) = 0. \quad (7)$$

Equation (7) can be cast into  $\partial_\mu j^\mu = 0$ , which represents the conservation of spin rooted in the  $U(1)$  spin-rotational symmetry of the Lagrangian about the  $z$  axis with

$$j^\mu = \sin^2 \theta \partial^\mu \phi. \quad (8)$$

The spin density and the spin current density are given by  $j^0$  and  $\mathbf{j} = (j^x, j^y)$ , respectively. Since the Lagrangian has no explicit dependence on space-time, the energy-momentum tensor in terms of  $\theta$  and  $\phi$ , which is given by

$$T^{\mu\nu} = \partial^\mu \theta \partial^\nu \theta + \sin^2 \theta \partial^\mu \phi \partial^\nu \phi - g^{\mu\nu} \mathcal{L}, \quad (9)$$

is also a conserved current satisfying the continuity equation  $\partial_\mu T^{\mu\nu} = 0$ .

The system can also be studied within the Hamiltonian formalism. Performing the Legendre transformation to the

Lagrangian yields the following Hamiltonian density:

$$\mathcal{H} = \frac{1}{2} \left[ \pi_\theta^2 + |\nabla\theta|^2 + \frac{\pi_\phi^2}{\sin^2\theta} + \sin^2\theta (|\nabla\phi|^2 + 1) \right], \quad (10)$$

where  $\pi_\theta \equiv \partial\mathcal{L}/\partial\dot{\theta} = \dot{\theta}$  and  $\pi_\phi \equiv \partial\mathcal{L}/\partial\dot{\phi} = \sin^2\theta\dot{\phi}$  are conjugate momenta of the fields  $\theta$  and  $\phi$ , respectively [82]. In the Hamiltonian formalism, the time evolution of fields or momenta is determined by their Poisson brackets with the system's Hamiltonian, which leads us to the same Eqs. (6) and (7) as in the Lagrangian formalism. See Appendix A for the derivation based on the Hamiltonian formalism.

### B. Skyrmion-textured domain walls

To obtain a static domain-wall solution, we set  $\dot{\theta} = 0$  and  $\dot{\phi} = 0$  in the equations of motion:

$$\nabla^2\theta - \sin\theta \cos\theta (\nabla\phi \cdot \nabla\phi + 1) = 0, \quad (11)$$

$$\nabla \cdot (\sin^2\theta \nabla\phi) = 0. \quad (12)$$

For a domain wall, we consider the following ansatz by employing separation of variables:

$$\theta(x, y) = \theta(x), \quad \phi(x, y) = \phi(y), \quad (13)$$

$$\mathbf{n}(x = \pm\infty, y) = \pm\hat{z}. \quad (14)$$

The equations are solved by the following solution:

$$\cos\theta = \tanh(\sqrt{1+k_0^2}x), \quad \phi = k_0y. \quad (15)$$

Here,  $k_0$  is a real number which characterizes chirality of the domain-wall texture. The chirality constant  $k_0$  gives rise to winding of the order parameter  $\mathbf{n}$  on the domain-wall line ( $x = 0$ ). The domain wall interpolates two discrete vacua  $\mathbf{n}(x, y) = \pm\hat{z}$ . In a two-dimensional system, a domain wall is a one-dimensional object which can exhibit nontrivial textures along with it [83,84]. With the considered solution, domain-wall angle  $\phi$  varies uniformly along the domain wall (i.e., along the  $y$  axis, see Fig. 1), which gives rise to the finite skyrmion charge density given by

$$\rho_{\text{sky}}(x, y) \equiv \frac{1}{4\pi} \mathbf{n} \cdot (\partial_x \mathbf{n} \times \partial_y \mathbf{n}) \quad (16)$$

$$= -\frac{k_0}{4\pi} (1+k_0^2) \text{sech}^2(\sqrt{1+k_0^2}x). \quad (17)$$

Note that the domain wall carries the skyrmion charge density, which is localized in the vicinity of the domain wall. Along the  $y$  axis, the density is uniform and the linear skyrmion charge density (per unit length in the  $y$  direction) is given by

$$\int dx \rho_{\text{sky}} = -\frac{k_0}{2\pi}. \quad (18)$$

If the periodic boundary condition along the  $y$  axis is demanded ( $y + L = y$ ), we would have  $\phi(L) = \phi(0)$ , which discretizes the allowed values for  $k_0$  as  $k_0 = 2\pi n/L$  for an integer  $n$ . The integration of the density yields the integer skyrmion charge  $\int dx dy \rho_{\text{sky}} = -n$  [61]. In the case of  $k_0 = 0$ , the domain-wall profile along the  $y$  axis is uniform and the corresponding skyrmion charge is zero.

For the static field, the Hamiltonian density is given by  $\mathcal{H} = -\mathcal{L}$ . The explicit expression for the energy density of the domain-wall solution (15) is given by

$$\mathcal{H} = (1+k_0^2) \text{sech}^2(\sqrt{1+k_0^2}x). \quad (19)$$

The energy density per unit length in the  $y$  axis is given by

$$E = \int dx \mathcal{H} = 2(1+k_0^2)^{\frac{1}{2}}. \quad (20)$$

Note that the nontrivial magnetic texture on the domain wall increases the energy.

We make one remark from Derrick's scaling argument [85]. Without  $n$ th-order derivative terms ( $n > 2$  or  $n = 1$ ) in the energy functional, finite energy isolated skyrmions are unstable in the bulk. However, skyrmions in a domain wall can be stable since the scaling argument is applied to the dimension perpendicular to the domain wall and to other dimensions separately [43,49,84]. In this paper, first, the characteristic length of the domain wall is determined by the ratio of  $A$  and  $K$  in the Lagrangian (1). Second, the characteristic length of the chiral texture in the domain wall is determined by the chirality constant  $k_0$ .

Experimentally, the obtained domain-wall states with the finite skyrmion charge can be realized by injecting a spin current into the magnet via the spin Hall effects as shown in Ref. [86] for a ferromagnet and in Refs. [87,88] for an antiferromagnet.

## III. SPIN WAVES ON TOP OF THE SKYRMION-TEXTURED DOMAIN WALL

In this section, we formulate the dynamics of magnons on top of the skyrmion-textured domain wall. With the aid of SUSY QM, we find chiral bound modes. Furthermore, we obtain an analytic form of a reflection probability of the magnon and show their refraction in the presence of the skyrmionic texture of the domain wall. This refraction is interpreted from the perspective of the emergent magnetic field for magnons.

### A. Spin waves

To obtain a spin-wave solution on top of the skyrmionic domain wall, we consider a small fluctuation  $\delta\mathbf{n}(\mathbf{x}, t)$  on the static domain-wall background  $\mathbf{n}(x)$  [Eq. (15)]. The variation of the vector is described by variations of the angles:

$$\delta n_1 = \delta\theta, \quad \delta n_2 = \sin\theta\delta\phi. \quad (21)$$

Linearizing the Euler-Lagrange equations [Eqs. (6) and (7)] with respect to the variation  $(\theta, \phi) \mapsto (\theta + \delta\theta, \phi + \delta\phi)$ , we obtain two coupled equations for  $\delta n_1$  and  $\delta n_2$ . The two equations are combined into one complex equation:

$$[\square + (1+k_0^2)(1-2\sin^2\theta) + 2qik_0 \cos\theta\partial_y] \Psi_q = 0, \quad (22)$$

where  $\Psi_q \equiv \delta n_1 - qi\delta n_2$ ,  $q = \pm 1$ , and  $\square \equiv \partial_\mu \partial^\mu$ . Here, the complex field  $\Psi_q$  represents  $q$ -polarized spin waves, where  $q = 1$  and  $-1$  are for right-handed and left-handed spin waves, respectively [89]. Since the Lagrangian for the antiferromagnet (2) is Lorentz invariant, the equation of motion for  $\Psi_q$  (22) is Lorentz invariant. For the case of ferromagnets, the Lagrangian is similar but nonrelativistic and the magnon

wave function has only a first-order time derivative in the equation of motion [62]. Due to the translational symmetries with respect to  $(t, y) \mapsto (t + \delta t, y + \delta y)$ , the equation

$$\Psi_q(t, x, y) = \psi_q(x)e^{i(k_y y - \omega t)} \quad (23)$$

is supported as an eigenfunction. The equation of motion for the eigenfunction is given by

$$\omega^2 \psi_q = \left[ -\partial_x^2 + k_y^2 + (1 + k_0^2)(1 - 2 \sin^2 \theta) - 2qk_0 k_y \cos \theta \right] \psi_q. \quad (24)$$

We interpret the equation as the ‘‘Schrödinger’’ equation  $\omega^2 \psi_q = H \psi_q$  with the eigenvalue  $\omega^2$  and the ‘‘Hamiltonian’’  $H = -\partial_x^2 + V$ , which consists of the kinetic energy  $-\partial_x^2$  and the potential energy given by

$$V = k_y^2 + (1 + k_0^2) \left[ 1 - 2 \operatorname{sech}^2(\sqrt{1 + k_0^2} x) \right] - 2qk_0 k_y \tanh(\sqrt{1 + k_0^2} x). \quad (25)$$

Equation (22) with the potential (25) is one of our main results. Here, the potential energy  $V$  is known as the Rosen-Morse potential [90]. Note that, for the case of the nontextured domain wall  $k_0 = 0$ , the potential becomes the Pöschl-Teller potential [91] which is known as a reflectionless potential [92]. In general, with nonzero  $k_0$ , spin waves are reflected; the derivation of the reflection probability is presented below in Sec. III D.

## B. SUSY QM

In this section, we solve the equation of motion for the spin wave with the aid of SUSY QM. To apply SUSY QM, we define the annihilation and creation operators:

$$a = \partial_x + \sqrt{1 + k_0^2} \tanh(\sqrt{1 + k_0^2} x) + \beta, \quad (26)$$

$$a^\dagger = -\partial_x + \sqrt{1 + k_0^2} \tanh(\sqrt{1 + k_0^2} x) + \beta, \quad (27)$$

where  $\beta = -qk_y k_0 / \sqrt{1 + k_0^2}$ . The commutation relation of the operators is given by

$$[a, a^\dagger] = 2(1 + k_0^2) \operatorname{sech}(\sqrt{1 + k_0^2} x). \quad (28)$$

With these operators, the Hamiltonian is written as  $H = a^\dagger a - \beta^2 + k_y^2$  and the SUSY partner Hamiltonian is defined as  $\tilde{H} = a a^\dagger - \beta^2 + k_y^2$ . The SUSY partner of the potential is defined by the relation  $\tilde{H} = -\partial_x^2 + \tilde{V}$ . Since, by definition,  $\tilde{H} = H + [a, a^\dagger]$ , the commutator (28) eliminates the sech term in the potential (25). Thus the induced partner potential is simpler than the original potential, that is,

$$\tilde{V} = k_y^2 + 1 + k_0^2 - 2qk_0 k_y \tanh(\sqrt{1 + k_0^2} x). \quad (29)$$

Figure 2 provides comparison of the original potential  $V$  and the partner potential  $\tilde{V}$ . Note that the partner potential for the case of  $k_0 = 0$  is a constant potential. Due to the algebraic

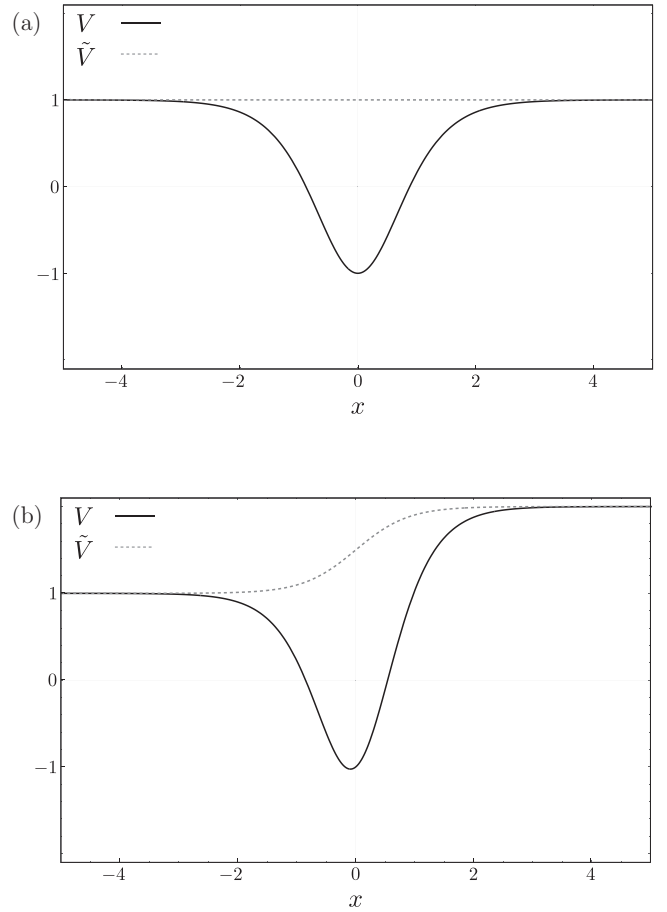


FIG. 2. The solid line represents the original potential (25) and the dashed line represents the SUSY partner (29). Here, we consider the case of left-polarized magnons ( $q = -1$ ) coming from the left  $x < 0$ . The chiralities of the skyrmion-textured domain wall are (a)  $k_0 = 0$  and (b)  $k_0 = 0.5$ , where  $k_y = k_0$ .

relation of  $H$  and  $\tilde{H}$ , eigenfunctions for both Hamiltonians satisfy the following relations:

$$\tilde{H} a \psi_q = a H \psi_q = \omega^2 a \psi_q, \quad (30)$$

$$H a^\dagger \tilde{\psi}_q = a^\dagger \tilde{H} \tilde{\psi}_q = \tilde{\omega}^2 a^\dagger \tilde{\psi}_q, \quad (31)$$

where  $\tilde{H} \tilde{\psi}_q = \tilde{\omega}^2 \tilde{\psi}_q$ . It means that  $a \psi_q (a^\dagger \tilde{\psi}_q)$  is an eigenfunction of  $\tilde{H} (H)$ . We will solve the problem in the partner system which is easier than the original system and obtain the solution for the original problem by applying the ladder operator,  $\psi_q = a^\dagger \tilde{\psi}_q$ .

## C. Domain-wall bound spin waves

Before elucidating propagating modes, we will discuss bound modes. Since the bound modes satisfy relation  $a \psi_q = 0$ , the solution is given by

$$\psi_q(x) = \operatorname{sech}(\sqrt{1 + k_0^2} x) e^{-\beta x}, \quad (32)$$

whose bound frequency is  $\omega^2 = -\beta^2 + k_y^2$ . The solution for bound modes is one of our main results. Note that, in this paper, the bound magnon propagates to the  $y$  direction whereas

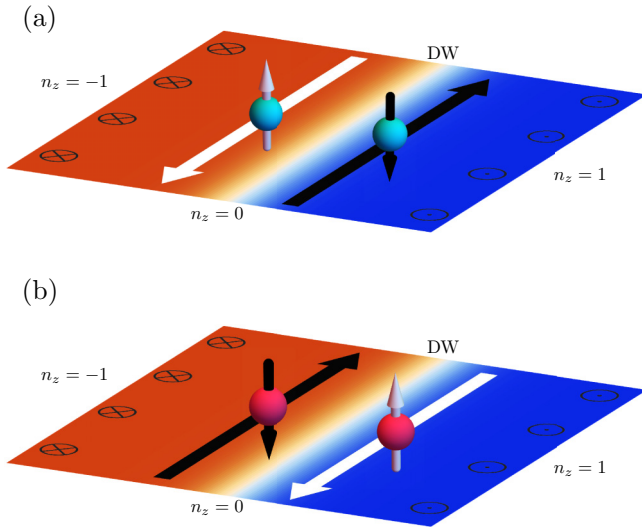


FIG. 3. Trajectories of (a) left-polarized bound magnons and (b) right-polarized bound magnons. Here  $k_0$  is assumed to be positive. The arrows piercing the balls represent the spins of the magnons. The arrows on the plane indicate the direction of the spin current due to the bound magnons.

it is localized in the  $x$  direction. Our solution generalizes the well-known bound solution [93] which corresponds to the case of  $\beta = 0$ . One can define the bound magnon's position as the location where the amplitude of the wave function is maximized. By this definition, the position of the bound magnon is given by

$$X = -\frac{q}{\sqrt{1+k_0^2}} \tanh^{-1} \left( \frac{k_y k_0}{1+k_0^2} \right). \quad (33)$$

Equation (33) tells us that positions of bound modes with different  $k_y$  are separated and left- and right-polarized bound magnons have opposite positions. Figure 3 schematically illustrates the trajectories of left- and right-polarized bound magnons.

#### D. Propagating spin waves

In the partner system described by  $\tilde{H}$ , asymptotic behaviors of the propagating wave function are

$$\tilde{\psi}_q(x \rightarrow -\infty) \sim e^{ik_-x} + r e^{-ik_-x}, \quad (34)$$

$$\tilde{\psi}_q(x \rightarrow +\infty) \sim t e^{ik_+x}, \quad (35)$$

where  $k_+^2 = k_-^2 - 4k_0k_y$  (from the conservation of the energy) and  $k_-$  is the wave number of the incoming spin wave. By acting of  $a^\dagger$  on  $\tilde{\psi}_q$ , asymptotic behaviors of the propagating wave function in the original system are given by

$$a^\dagger \tilde{\psi}_q(x \rightarrow -\infty) \sim [-ik_- - 2k_0k_y + \beta] e^{ik_-x} + r[ik_- - 2k_0k_y + \beta] e^{-ik_-x}, \quad (36)$$

$$a^\dagger \tilde{\psi}_q(x \rightarrow +\infty) \sim t[-ik_+ + 2k_0k_y + \beta] e^{ik_+x}. \quad (37)$$

Reflection probability of the original potential is

$$\mathfrak{R} = \left| \frac{ik_- - 2k_0k_y + \beta}{-ik_- - 2k_0k_y + \beta} \right|^2 |r|^2 = |r|^2, \quad (38)$$

and it is known to be equivalent to the reflection probability of the partner potential from SUSY QM. The partner system has the hyperbolic-tangent potential which is known to be solvable. The transmission probability  $\mathfrak{T} = 1 - \mathfrak{R}$  is given by [64,94,95]

$$\mathfrak{T}(k_-, k_y) = \left[ 1 - \frac{\sinh^2 \left[ \frac{\pi(k_+ - k_-)}{2\sqrt{1+k_0^2}} \right]}{\sinh^2 \left[ \frac{\pi(k_+ + k_-)}{2\sqrt{1+k_0^2}} \right]} \right] \Theta(k_-^2 - 4k_0k_y), \quad (39)$$

where  $\Theta$  is the Heaviside step function. To capture the deflection of a magnon trajectory in real space, we express the wave function in the laboratory frame  $\{\hat{x}, \hat{y}, \hat{z}\}$ :

$$\begin{aligned} \psi_{\text{lab}}^{\text{in}} &= \delta \mathbf{n} \cdot (\hat{x} - i\hat{y}) = (-1)\Psi e^{-ik_0y} \quad \text{as } x \rightarrow -\infty \\ &\sim \psi(x) e^{i(k_y - k_0)y - \omega t}, \\ \psi_{\text{lab}}^{\text{out}} &= \delta \mathbf{n} \cdot (\hat{x} + i\hat{y}) = \Psi e^{ik_0y} \quad \text{as } x \rightarrow +\infty \\ &\sim \psi(x) e^{i(k_y + k_0)y - \omega t}, \end{aligned} \quad (40)$$

where the extra factor  $\exp(\pm ik_0y)$  comes from the fact that  $\Psi$  is defined with respect to the local spin frame where the azimuthal angle changes along the  $y$  direction in the domain wall. For concreteness of discussion, let us first consider left-polarized magnons. Note that the  $y$  component of the magnon's linear momentum is changed from  $k_y - k_0$  to  $k_y + k_0$  after passing by the domain wall. In the laboratory frame, wave vectors of incoming, reflected, and transmitted magnons with left-handed polarization are given by

$$\mathbf{k}^L = (k_-, k_y - k_0, 0), \quad (41)$$

$$\mathbf{k}_r^L = (-k_-, k_y - k_0, 0), \quad (42)$$

$$\mathbf{k}_t^L = (k_+, k_y + k_0, 0). \quad (43)$$

In the laboratory frame, the kinetic energy of magnons is conserved, which ensures the following equalities:  $|\mathbf{k}| = |\mathbf{k}_r| = |\mathbf{k}_t|$ . Let us consider a magnon incoming from  $x < 0$  along the  $x$  axis. This is the case of  $k_y - k_0 = 0$ . This magnon initially has no  $y$  component of the wave vector. However, after the transmission through the domain wall, the magnon has nonzero  $y$  component  $2k_0$ . For magnons with right-handed polarization, reflection direction is opposite. Wave vectors of incoming, reflected, and transmitted right-polarized magnons are

$$\mathbf{k}^R = (k_-, k_y + k_0, 0), \quad (44)$$

$$\mathbf{k}_r^R = (-k_-, k_y + k_0, 0), \quad (45)$$

$$\mathbf{k}_t^R = (k_+, k_y - k_0, 0). \quad (46)$$

Expanding the spin density  $j^0(\theta, \phi)$  (8) with respect to  $(\theta \rightarrow \theta + \delta\theta, \phi \rightarrow \phi + \delta\phi)$  up to second order, we can obtain the spin of  $q$ -polarized magnons. Since unperturbed fields  $\theta$  and  $\phi$  are time independent, the zeroth order of the spin

density is zero. Using the definition (21), we expand the spin density:

$$\begin{aligned} j^0 &= \sin^2 \theta \partial_t \delta \phi + 2 \sin \theta \cos \theta \delta \theta \partial_t \delta \phi \\ &= \sin \theta \partial_t \delta n_2 + 2 \cos \theta \delta n_1 \partial_t \delta n_2. \end{aligned} \quad (47)$$

From the following expression of the magnon wave function (23)

$$\Psi_q(t, x, y) = \delta n_1 - qi \delta n_2 = |\psi_q(x)| e^{i(k_y y - \omega t + \eta)}, \quad (48)$$

the perturbative fields read as

$$\begin{aligned} \delta n_1 &\propto \cos(k_y y - \omega t + \eta), \\ \delta n_2 &\propto -q \sin(k_y y - \omega t + \eta), \end{aligned} \quad (49)$$

where  $\eta$  is an arbitrary phase. Plugging Eq. (49) into Eq. (47) and evaluating its expectation value with respect to time averaging, the first-order term vanishes and the remaining term yields

$$\langle j^0 \rangle_t \propto q \omega \cos \theta = q \omega \tanh(\sqrt{1 + k_0^2} x). \quad (50)$$

This equation indicates that spin of the left-polarized (right-polarized) magnon is changed from  $+(−)\hbar$  to  $−(+)\hbar$  while the magnon is passing through the domain wall.

### E. Perspective of emergent electromagnetism

Here, we describe an alternative way to understand the deflection of a magnon trajectory by invoking the emergent electromagnetism of spin waves on top of a magnetic texture. From the second-order variation of the Lagrangian of the antiferromagnets, we obtain the Lagrangian of the magnon:

$$\mathcal{L}_{\text{SW}} = \frac{1}{2} (D_\mu \Psi_q)^* (D^\mu \Psi_q), \quad (51)$$

where the covariant derivatives and texture-induced gauge field are given by [89,96]

$$D_\mu = \partial_\mu + iqa_\mu, \quad a_\mu = -\cos \theta \partial_\mu \phi. \quad (52)$$

Detailed derivation of the Lagrangian can be found in Appendix B. The covariant derivative and the gauge field for the magnon are expected by the notion of the connection in differential geometry since the magnon lives on the tangent space of the sphere [97,98]. From the given domain-wall solution (15), the emergent magnetic field is obtained by [69]

$$\begin{aligned} b &= -(\partial_1 a_2 - \partial_2 a_1) \\ &= k_0 \sqrt{1 + k_0^2} \text{sech}^2(\sqrt{1 + k_0^2} x). \end{aligned} \quad (53)$$

The change of the transverse momentum due to the emergent Lorentz force is given by

$$\Delta p_y = \int q(\mathbf{v} \times \mathbf{b}) \cdot \hat{y} dt = -2qk_0, \quad (54)$$

where  $\mathbf{v}$  is the magnon velocity and  $\mathbf{b} = b\hat{z}$ . This result is consistent with the result obtained by SUSY QM. Note that the change of the transverse momentum depends on the polarization  $q$  of the magnon. This indicates that, when the same number of two distinctly polarized magnons pass the skyrmion-textured domain wall in the longitudinal direction (e.g.,  $x$  direction), there arises a net finite spin current while

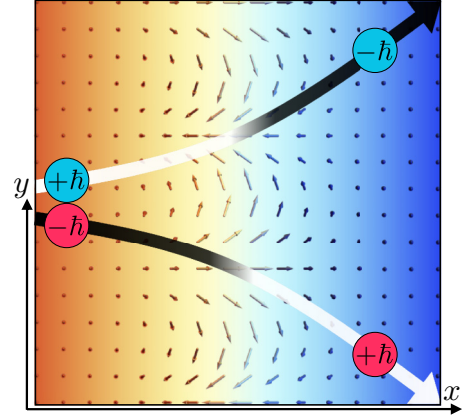


FIG. 4. Schematic illustration of the motion of distinctly polarized antiferromagnetic magnons moving across the skyrmion-textured domain wall. Similar to Fig. 3, the blue (red) ball represents the left-polarized (right-polarized) magnon and the color change of the arrow depicts the change of spin angular momentum of the magnon passing through the domain wall [the change from white (black) to black (white) represents the change from  $+(−)\hbar$  to  $−(+)\hbar$ ]. Note that, when the same number of two distinctly polarized magnons move in the longitudinal direction, the resultant net transverse magnon current vanishes, but the net transverse spin current is finite.

having a zero net magnon current in the transverse direction (e.g.,  $y$  direction). The situation is illustrated in Fig. 4.

### IV. TUNABLE THERMAL TRANSPORT

In this section, we obtain the chirality-dependent thermal transport. The injected spin current at the boundary which is electronically tunable via the spin Hall effect determines mathematical boundary conditions of the system. Thus we can control the chirality of the texture that is represented by  $k_0$  (15). To compute the tunable heat flux, we use the Landauer-Büttiker formula [99–101]. Heat flux per unit length is given by

$$\begin{aligned} \mathcal{J} &= \sum_q \int_0^\infty \frac{dk_x}{2\pi} \int_{-\infty}^\infty \frac{dk_y}{2\pi} \mathfrak{T}(k_x, k_y) \hbar \\ &\times \left[ \omega_{qL} n(\omega_{qL}, T_L) \frac{\partial \omega_{qL}}{\partial k_x} - \omega_{qR} n(\omega_{qR}, T_R) \frac{\partial \omega_{qR}}{\partial k_x} \right], \end{aligned} \quad (55)$$

where  $\omega_{qL(R)}$  is the frequency of a  $q$ -polarized magnon at the left (right) domain  $x < 0$  ( $x > 0$ ),  $T_{L(R)}$  is the temperature of the left (right) domain, and  $n(\omega, T)$  is the Bose-Einstein distribution. Figure 5 shows chirality dependence of the heat flow.  $\tilde{T}_{L(R)} \equiv k_B T_{L(R)} / \hbar$  is a rescaled temperature. Note that we use the natural unit  $\rho = K = A = 1$ . Therefore time, length, and energy are measured by  $\sqrt{\rho/K}$ ,  $\sqrt{A/K}$ , and  $A$ , respectively. As we expected, chirality of the skyrmion-textured domain wall disturbs the longitudinal magnon transport.

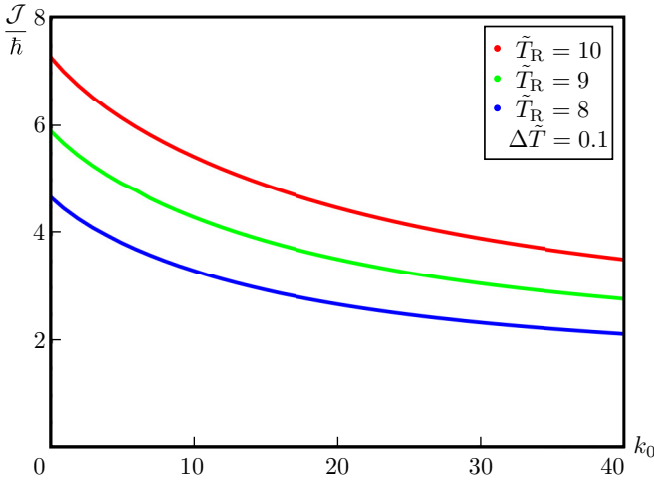


FIG. 5. Chirality dependence of the heat flux. Here,  $\tilde{T}_R$  denotes the rescaled temperature of the right reservoir and the temperature difference between two reservoirs is fixed as  $\Delta\tilde{T} = 0.1$ , where  $\tilde{T}_L - \tilde{T}_R \equiv \Delta\tilde{T}$ .

## V. CONCLUSION

We have formulated a theory of the skyrmion-textured domain wall in a two-dimensional antiferromagnet. Using the Lagrangian formalism, we have derived equations of motion for magnons on top of the skyrmion-textured domain wall. Using SUSY QM, we have obtained the exact solutions of magnon bound modes and investigated their scattering

properties in the skyrmion-textured domain wall. With the chiral texture, the domain-wall potential is no longer symmetric under the space inversion, and thus the position of the bound magnon is shifted from the domain-wall center. Solving the scattering problem of the domain-wall potential for magnons, we have shown that magnons are refracted or reflected due to the chiral texture of the domain wall. This refraction can be interpreted as the magnon dynamics under the emergent electromagnetism. Using the gauged sigma model approach, we also have analyzed the Lagrangians of the magnet and the magnon and find how the effective electromagnetism for the magnons emerges in the chiral texture of the background magnet. We have found the total reflection of magnons which lack enough longitudinal momentum to overcome the domain-wall potential. The total reflection and the chirality-proportional reflection probability which can be tuned electronically reduce the thermal transport.

## ACKNOWLEDGMENTS

This work was supported by the Brain Pool Plus Program through the National Research Foundation of Korea (NRF) funded by the Ministry of Science and ICT (Grant No. NRF-2020H1D3A2A03099291), an NRF grant funded by the Korea government (Grant No. NRF-2021R1C1C1006273), and National Research Foundation of Korea funded by the Korea Government via the SRC Center for Quantum Coherence in Condensed Matter (Grant No. NRF-2016R1A5A1008184). K.N. acknowledges support by Japan Society for the Promotion of Science KAKENHI Grants No. JP20K14420 and No. JP22K03519.

## APPENDIX A: EQUATIONS OF MOTION FROM POISSON BRACKETS

Poisson brackets of the fields and its momenta are

$$\{\varphi_a(\mathbf{x}, t), \varphi_b(\mathbf{x}', t)\} = 0, \quad (\text{A1})$$

$$\{\pi_a(\mathbf{x}, t), \pi_b(\mathbf{x}', t)\} = 0, \quad (\text{A2})$$

$$\{\varphi_a(\mathbf{x}, t), \pi_b(\mathbf{x}', t)\} = \delta_{ab}\delta(\mathbf{x} - \mathbf{x}'). \quad (\text{A3})$$

Here, indices  $a$  and  $b$  denote the fields  $\theta$  and  $\phi$ . With these canonical relations, equations of motion for the fields are driven, since time evolution is given by a Poisson bracket with the Hamiltonian. For  $\theta$  and  $\pi_\theta$ , time evolutions are

$$\dot{\theta} = \{\theta, H\} = \int d^2x' \{\theta(\mathbf{x}), \mathcal{H}\} = \int d^2x' \left\{ \theta(\mathbf{x}), \frac{1}{2} \pi_\theta^2 \right\} = \int d^2x' \{\theta(\mathbf{x}), \pi_\theta\} \pi_\theta = \int d^2x' \delta(\mathbf{x} - \mathbf{x}') \pi_\theta(\mathbf{x}') \quad (\text{A4})$$

$$= \pi_\theta, \quad (\text{A5})$$

$$\dot{\pi}_\theta = \{\pi_\theta, H\} = \int d^2x' \{\pi_\theta(\mathbf{x}), \mathcal{H}\} \quad (\text{A6})$$

$$= \int d^2x' \left[ \left\{ \pi_\theta(\mathbf{x}), \frac{1}{2} \nabla\theta \cdot \nabla\theta \right\} + \left\{ \pi_\theta(\mathbf{x}), \frac{1}{2} \frac{\pi_\phi^2}{\sin^2\theta} \right\} + \left\{ \pi_\theta(\mathbf{x}), \frac{1}{2} \sin^2\theta \right\} (\nabla\phi \cdot \nabla\phi + 1) \right] \quad (\text{A7})$$

$$= \int d^2x' \left[ \nabla^2\theta(\mathbf{x}') \delta(\mathbf{x} - \mathbf{x}') + \pi_\phi^2 \frac{\cos\theta}{\sin^3\theta} \delta(\mathbf{x} - \mathbf{x}') - \sin\theta \cos\theta (\nabla\phi \cdot \nabla\phi + 1) \delta(\mathbf{x} - \mathbf{x}') \right] \quad (\text{A8})$$

$$= \nabla^2\theta + \sin\theta \cos\theta (\dot{\phi}^2 - \nabla\phi \cdot \nabla\phi - 1). \quad (\text{A9})$$

Since  $\dot{\pi}_\phi = \dot{\theta}$ , Eq. (A9) is consistent with Eq. (6). Similarly equations for  $\phi$  and  $\pi_\phi$  are

$$\dot{\phi} = \{\phi, H\} = \int d^2x' \{\phi(\mathbf{x}), \mathcal{H}\} = \int d^2x' \left\{ \phi(\mathbf{x}), \frac{\pi_\phi^2}{2 \sin^2 \theta} \right\} = \int d^2x' \delta(\mathbf{x} - \mathbf{x}') \frac{1}{\sin^2 \theta} \pi_\phi \quad (\text{A10})$$

$$= \frac{\pi_\phi}{\sin^2 \theta}, \quad (\text{A11})$$

$$\dot{\pi}_\phi = \{\pi_\phi, H\} = \int d^2x' \{\pi_\phi(\mathbf{x}), \mathcal{H}\} \quad (\text{A12})$$

$$= \int d^2x' \left\{ \pi_\phi(\mathbf{x}), \frac{1}{2} \sin^2 \theta \nabla \phi \cdot \nabla \phi \right\} = \int d^2x' \sin^2 \theta \sum_i \{\pi_\phi(\mathbf{x}), \partial_i \phi\} \partial_i \phi \quad (\text{A13})$$

$$= \int d^2x' \sin^2 \theta \sum_i (-1) \partial_i \delta(\mathbf{x} - \mathbf{x}') \partial_i \phi = \int d^2x' \sum_i \delta(\mathbf{x} - \mathbf{x}') \partial_i (\sin^2 \theta \partial_i \phi) \quad (\text{A14})$$

$$= \int d^2x' \delta(\mathbf{x} - \mathbf{x}') \nabla \cdot (\sin^2 \theta \nabla \phi) \quad (\text{A15})$$

$$= \nabla \cdot (\sin^2 \theta \nabla \phi). \quad (\text{A16})$$

Since  $\pi_\phi = \sin^2 \theta \dot{\phi}$ , Eq. (A16) is identical to Eq. (7).

## APPENDIX B: SECOND VARIATION OF THE LAGRANGIAN

The Néel vector is a unit vector on the sphere  $S^2$ . Thus the Néel vector can be written as a rotation of a constant unit vector

$$\mathbf{n}(\mathbf{x}, t) = \mathcal{R}(\mathbf{x}, t) \mathbf{e} \quad (\text{B1})$$

where the rotation matrix is defined by

$$\mathcal{R} = e^{\phi(\mathbf{x}, t) L_z} e^{\theta(\mathbf{x}, t) L_y}, \quad (\text{B2})$$

and the generators are

$$L_x = \begin{pmatrix} 0 & 0 & 0 \\ 0 & 0 & -1 \\ 0 & 1 & 0 \end{pmatrix}, \quad L_y = \begin{pmatrix} 0 & 0 & 1 \\ 0 & 0 & 0 \\ -1 & 0 & 0 \end{pmatrix}, \quad L_z = \begin{pmatrix} 0 & -1 & 0 \\ 1 & 0 & 0 \\ 0 & 0 & 0 \end{pmatrix}. \quad (\text{B3})$$

With this representation, the derivative of the Néel vector is written as

$$\partial_\mu \mathbf{n} = [(\partial_\mu \mathcal{R}) + \mathcal{R} \partial_\mu] \mathbf{e} \quad (\text{B4})$$

$$= \mathcal{R} [\mathcal{R}^{-1} (\partial_\mu \mathcal{R}) + \partial_\mu] \mathbf{e} \quad (\text{B5})$$

$$\equiv \mathcal{R} [\mathcal{A}_\mu + \partial_\mu] \mathbf{e}. \quad (\text{B6})$$

The Lagrangian density of the Heisenberg antiferromagnet is given by

$$\mathcal{L} = \frac{1}{2} \partial_\mu \mathbf{n} \cdot \partial^\mu \mathbf{n}, \quad (\text{B7})$$

and this is called the O(3) sigma model. Plugging Eq. (B6) into the Lagrangian (B7), we can obtain the gauged sigma model:

$$\mathcal{L} = \frac{1}{2} \partial_\mu \mathbf{n} \cdot \partial^\mu \mathbf{n} \quad (\text{B8})$$

$$= \frac{1}{2} \mathcal{R} [\partial_\mu + \mathcal{A}_\mu] \mathbf{e} \cdot \mathcal{R} [\partial^\mu + \mathcal{A}^\mu] \mathbf{e} \quad (\text{B9})$$

$$= \frac{1}{2} [\partial_\mu + \mathcal{A}_\mu] \mathbf{e} \cdot [\partial^\mu + \mathcal{A}^\mu] \mathbf{e} \quad (\text{B10})$$

$$= \frac{1}{2} \mathcal{D}_\mu \mathbf{e} \cdot \mathcal{D}^\mu \mathbf{e}, \quad (\text{B11})$$

with the covariant derivative

$$\mathcal{D}_\mu \equiv \partial_\mu + \mathcal{A}_\mu, \quad (\text{B12})$$

and the SO(3) gauge field  $\mathcal{A}_\mu \in \text{so}(3)$ , where  $\text{so}(3)$  is the Lie algebra of the Lie group SO(3). Since the rotation generators (B3) form a basis of  $\text{so}(3)$ , we can write the covariant derivative as

$$\mathcal{D}_\mu = \partial_\mu + \mathcal{A}_\mu = \partial_\mu + A_\mu^i L_i, \quad (\text{B13})$$

$$[\mathcal{D}_\mu \mathbf{e}]^j = \partial_\mu [\mathbf{e}]^j + A_\mu^i [L_i]^j_k [\mathbf{e}]^k = \partial_\mu [\mathbf{e}]^j + A_\mu^i \epsilon_{ik}^j [\mathbf{e}]^k = [\partial_\mu \mathbf{e} - \mathbf{A}_\mu \times \mathbf{e}]^j, \quad (\text{B14})$$

where  $A_\mu^i$  is the  $i$ th component of  $\mathbf{A}_\mu$  which is the dual vector of  $\mathcal{A}_\mu$  and  $\epsilon$  is the Levi-Civita tensor. In Ref. [102], the author uses  $\mathbf{A}_\mu$  as a SO(3) gauge field. The gauge field  $\mathcal{A}_\mu$  and its dual  $\mathbf{A}_\mu$  have the same information and are linked by the relation

$$[\mathcal{A}_\mu]_j^i = \epsilon_{jk}^i A_\mu^k. \quad (\text{B15})$$

Effects of magnons are captured by the expansion of  $\mathbf{e} \approx \hat{z} + \delta\mathbf{e}$ , where  $\delta\mathbf{e} = \delta e_1 \hat{x} + \delta e_2 \hat{y}$ ,  $|\delta\mathbf{e}| \ll 1$ . We will obtain the Lagrangian of a magnon via the second-order variation with respect to  $\delta\mathbf{e}$ . The expansion of the Lagrangian is written as

$$2\mathcal{L} = \mathcal{D}_\mu \mathbf{e} \cdot \mathcal{D}^\mu \mathbf{e} \quad (\text{B16})$$

$$= \mathcal{A}_\mu \mathbf{e} \cdot \mathcal{A}^\mu \mathbf{e} + \partial_\mu \mathbf{e} \cdot \partial^\mu \mathbf{e} + 2\mathcal{A}_\mu \mathbf{e} \cdot \partial^\mu \mathbf{e} \quad (\text{B17})$$

$$= \mathcal{A}_\mu \hat{z} \cdot \mathcal{A}^\mu \hat{z} + \mathcal{A}_\mu \delta\mathbf{e} \cdot \mathcal{A}^\mu \delta\mathbf{e} + 2\mathcal{A}_\mu \hat{z} \cdot \mathcal{A}^\mu \delta\mathbf{e} + \partial_\mu \delta\mathbf{e} \cdot \partial^\mu \delta\mathbf{e} + 2\mathcal{A}_\mu \delta\mathbf{e} \cdot \partial^\mu \delta\mathbf{e} + 2\mathcal{A}_\mu \hat{z} \cdot \partial^\mu \delta\mathbf{e}. \quad (\text{B18})$$

The zeroth-order term is the Lagrangian without the magnon and the first-order terms vanish due to the stationary action principle. Now, the Lagrangian of the magnon (spin wave) is obtained:

$$2\mathcal{L}_{\text{SW}} = \partial_\mu \delta\mathbf{e} \cdot \partial^\mu \delta\mathbf{e} + \mathcal{A}_\mu \delta\mathbf{e} \cdot \mathcal{A}^\mu \delta\mathbf{e} + 2\mathcal{A}_\mu \delta\mathbf{e} \cdot \partial^\mu \delta\mathbf{e} \quad (\text{B19})$$

$$= \partial_\mu \delta\mathbf{e} \cdot \partial^\mu \delta\mathbf{e} + [[\mathcal{A}_\mu]_2^1 \delta e_2 \hat{x} + [\mathcal{A}_\mu]_1^2 \delta e_1 \hat{y} + ([\mathcal{A}_\mu]_1^3 \delta e_1 + [\mathcal{A}_\mu]_2^3 \delta e_2) \hat{z}] \cdot \mathcal{A}^\mu \delta\mathbf{e} + 2\mathcal{A}_\mu \delta\mathbf{e} \cdot \partial^\mu \delta\mathbf{e} \quad (\text{B20})$$

$$= \partial_\mu \delta\mathbf{e} \cdot \partial^\mu \delta\mathbf{e} + [\mathcal{A}_\mu]_2^1 [\mathcal{A}^\mu]_2^1 \delta e_2 \delta e_2 + [\mathcal{A}_\mu]_1^2 [\mathcal{A}^\mu]_1^2 \delta e_1 \delta e_1 \quad (\text{B21})$$

$$+ ([\mathcal{A}_\mu]_1^3 \delta e_1 + [\mathcal{A}_\mu]_2^3 \delta e_2) ([\mathcal{A}^\mu]_1^3 \delta e_1 + [\mathcal{A}^\mu]_2^3 \delta e_2) \quad (\text{B22})$$

$$+ 2[\mathcal{A}_\mu]_2^1 \delta e_2 \partial^\mu \delta e_1 - 2[\mathcal{A}_\mu]_1^2 \delta e_1 \partial^\mu \delta e_2 \quad (\text{B23})$$

$$= \partial_\mu \delta\mathbf{e} \cdot \partial^\mu \delta\mathbf{e} + a_\mu a^\mu (\delta e_1 \delta e_1 + \delta e_2 \delta e_2) + 2a^\mu (\delta e_2 \partial_\mu \delta e_1 - \delta e_1 \partial_\mu \delta e_2) \quad (\text{B24})$$

$$+ ([\mathcal{A}_\mu]_1^3 \delta e_1 + [\mathcal{A}_\mu]_2^3 \delta e_2) ([\mathcal{A}^\mu]_1^3 \delta e_1 + [\mathcal{A}^\mu]_2^3 \delta e_2). \quad (\text{B25})$$

Here, we define the texture induced gauge field by the longitudinal component of  $\mathbf{A}_\mu$ :

$$a_\mu \equiv [\mathcal{A}_\mu]_2^1 = A_\mu^3, \quad (\text{B26})$$

which is dominant for the dynamics of high-energy magnons. Let us introduce a magnon wave function  $\Psi_q \equiv \delta e_1 - q i \delta e_2$ , and then the Lagrangian is written as

$$2\mathcal{L}_{\text{SW}} = \partial_\mu \Psi_q^* \partial^\mu \Psi_q + a_\mu a^\mu \Psi_q^* \Psi_q - i q a^\mu (\Psi_q^* \partial_\mu \Psi_q - \Psi_q \partial_\mu \Psi_q^*) \quad (\text{B27})$$

$$+ ([\mathcal{A}_\mu]_1^3 \delta e_1 + [\mathcal{A}_\mu]_2^3 \delta e_2) ([\mathcal{A}^\mu]_1^3 \delta e_1 + [\mathcal{A}^\mu]_2^3 \delta e_2), \quad (\text{B28})$$

$$= (D_\mu \Psi_q)^* (D^\mu \Psi_q) + ([\mathcal{A}_\mu]_1^3 \delta e_1 + [\mathcal{A}_\mu]_2^3 \delta e_2) ([\mathcal{A}^\mu]_1^3 \delta e_1 + [\mathcal{A}^\mu]_2^3 \delta e_2), \quad (\text{B29})$$

where the covariant derivative is defined as

$$D_\mu \equiv \partial_\mu + i q a_\mu. \quad (\text{B30})$$

In Eq. (B29), the covariant derivative term induces the  $k_\mu$  term while the last term does not. Here, we consider the high-energy magnon limit, which means that the background texture varies slowly and this is equivalent to the adiabatic approximation. In the high-energy-magnon limit, the derivative term in the Lagrangian is dominant, therefore we can neglect the last term. Hence the Lagrangian of the magnon is given by

$$\mathcal{L}_{\text{SW}} = \frac{1}{2} (D_\mu \Psi_q)^* (D^\mu \Psi_q). \quad (\text{B31})$$

If we add the anisotropy term to the Hamiltonian, then the length scale of field configurations is given by

$$\lambda = \sqrt{\frac{A}{K}}, \quad (\text{B32})$$

where  $A$  and  $K$  are exchange and anisotropy constants. For the adiabatic approximation,  $A \gg K$  and this is called the exchange approximation. Thus, in this limit, we discard the anisotropy term in the Lagrangian, even if the system has an anisotropy.

Let  $\{\mathbf{e}_i\}$  be a local frame corotating with the spin texture and let  $\{\mathbf{e}_j\}$  be a fixed global frame. The twist of the frame is given by

$$\mathbf{e}_i \cdot \partial_\mu \mathbf{e}_j = \mathcal{R} \mathbf{e}_i \cdot \partial_\mu \mathcal{R} \mathbf{e}_j \quad (\text{B33})$$

$$= \mathbf{e}_i \cdot \mathcal{R}^{-1} \partial_\mu \mathcal{R} \mathbf{e}_j \quad (\text{B34})$$

$$= \mathbf{e}_i \cdot \mathcal{A}_\mu \mathbf{e}_j \quad (\text{B35})$$

$$= [\mathcal{A}_\mu]_{ij}. \quad (\text{B36})$$

The local rotation of a basis  $\{\varepsilon_1, \varepsilon_2\}$  endows a local phase rotation of the complex scalar  $\Psi_q$ . Thus, naturally,  $[\mathcal{A}_\mu]_{12} = A_\mu^3$  becomes the U(1) gauge field for the complex scalar  $\Psi_q$  and generates the emergent electromagnetism.

- 
- [1] V. Baltz, A. Manchon, M. Tsoi, T. Moriyama, T. Ono, and Y. Tserkovnyak, Antiferromagnetic spintronics, *Rev. Mod. Phys.* **90**, 015005 (2018).
- [2] T. Jungwirth, X. Marti, P. Wadley, and J. Wunderlich, Antiferromagnetic spintronics, *Nat. Nanotechnol.* **11**, 231 (2016).
- [3] R. Cheng, M. W. Daniels, J.-G. Zhu, and D. Xiao, Ultrafast switching of antiferromagnets via spin-transfer torque, *Phys. Rev. B* **91**, 064423 (2015).
- [4] R. Khoshlahni, A. Qaiumzadeh, A. Bergman, and A. Brataas, Ultrafast generation and dynamics of isolated skyrmions in antiferromagnetic insulators, *Phys. Rev. B* **99**, 054423 (2019).
- [5] S. Gongyo, Y. Kikuchi, T. Hyodo, and T. Kunihiro, Effective field theory and the scattering process for magnons in ferromagnets, antiferromagnets, and ferrimagnets, *Prog. Theor. Exp. Phys.* **2016**, 083B01 (2016).
- [6] S. M. Rezende, A. Azevedo, and R. L. Rodríguez-Suárez, Introduction to antiferromagnetic magnons, *J. Appl. Phys.* **126**, 151101 (2019).
- [7] M. Hongo, T. Fujimori, T. Misumi, M. Nitta, and N. Sakai, Effective field theory of magnons: Chiral magnets and the Schwinger mechanism, *Phys. Rev. B* **104**, 134403 (2021).
- [8] X. S. Wang and X. R. Wang, Topological magnonics, *J. Appl. Phys.* **129**, 151101 (2021).
- [9] In our paper, we use two terms “spin wave” and “magnon” interchangeably with emphasis on wavelike and particlelike properties of magnetic excitations, respectively.
- [10] A. V. Chumak, V. I. Vasyuchka, A. A. Serga, and B. Hillebrands, Magnon spintronics, *Nat. Phys.* **11**, 453 (2015).
- [11] A. Barman, G. Gubbiotti, S. Ladak, A. O. Adeyeye, M. Krawczyk, J. Gräfe, C. Adelmann, S. Cotozana, A. Naeemi, V. I. Vasyuchka, B. Hillebrands, S. A. Nikitov, H. Yu, D. Grundler, A. V. Sadovnikov, A. A. Grachev, S. E. Sheshukova, J.-Y. Duquesne, M. Marangolo, G. Csaba, W. Porod, V. E. Demidov, S. Urazhdin, S. O. Demokritov, E. Albisetti, D. Petti, R. Bertacco, H. Schultheiss, V. V. Kruglyak, V. D. Poimanov, S. Sahoo, J. Sinha, H. Yang, M. Münzenberg, T. Moriyama, S. Mizukami, P. Landeros, R. A. Gallardo, G. Carlotti, J.-V. Kim, R. L. Stamps, R. E. Camley, B. Rana, Y. Otani, W. Yu, T. Yu, G. E. W. Bauer, C. Back, G. S. Uhrig, O. V. Dobrovolskiy, B. Budinska, H. Qin, S. van Dijken, A. V. Chumak, A. Khitun, D. E. Nikonov, I. A. Young, B. W. Zingsem, and M. Winklhofer, The 2021 magnonics roadmap, *J. Phys.: Condens. Matter* **33**, 413001 (2021).
- [12] G. E. W. Bauer, E. Saitoh, and B. J. van Wees, Spin caloritronics, *Nat. Mater.* **11**, 391 (2012).
- [13] N. Manton and P. Sutcliffe, *Topological Solitons*, Cambridge Monographs on Mathematical Physics (Cambridge University, Cambridge, England, 2004).
- [14] T. Vachaspati, *Kinks and Domain Walls: An Introduction to Classical and Quantum Solitons* (Cambridge University, Cambridge, England, 2006).
- [15] E. J. Weinberg, *Classical Solutions in Quantum Field Theory: Solitons and Instantons in High Energy Physics*, Cambridge Monographs on Mathematical Physics (Cambridge University, Cambridge, England, 2012).
- [16] Y. M. Shnir, *Topological and Non-Topological Solitons in Scalar Field Theories*, Cambridge Monographs on Mathematical Physics (Cambridge University, Cambridge, England, 2018).
- [17] M. Nitta, Relations among topological solitons, *Phys. Rev. D* **105**, 105006 (2022).
- [18] V. Vento, Skyrmions at high density, *Int. J. Mod. Phys. E* **26**, 1740029 (2017).
- [19] B.-Y. Park, W.-G. Paeng, and V. Vento, The inhomogeneous phase of dense skyrmion matter, *Nucl. Phys. A* **989**, 231 (2019).
- [20] P. J. Ackerman, J. van de Lagemaat, and I. I. Smalyukh, Self-assembly and electrostriction of arrays and chains of hopfion particles in chiral liquid crystals, *Nat. Commun.* **6**, 6012 (2015).
- [21] P. J. Ackerman and I. I. Smalyukh, Diversity of Knot Solitons in Liquid Crystals Manifested by Linking of Preimages in Torons and Hopfions, *Phys. Rev. X* **7**, 011006 (2017).
- [22] S. Afghah and J. V. Selinger, Theory of helicoids and skyrmions in confined cholesteric liquid crystals, *Phys. Rev. E* **96**, 012708 (2017).
- [23] C. Long, X. Tang, R. L. B. Selinger, and J. V. Selinger, Geometry and mechanics of disclination lines in 3D nematic liquid crystals, *Soft Matter* **17**, 2265 (2021).
- [24] C. Long and J. V. Selinger, Coarse-grained theory for motion of solitons and skyrmions in liquid crystals, *Soft Matter* **17**, 10437 (2021).
- [25] C. D. Schimming and J. Viñals, Singularity identification for the characterization of topology, geometry, and motion of nematic disclination lines, *Soft Matter* **18**, 2234 (2022).
- [26] C. D. Schimming and J. Viñals, Anisotropic disclination cores in nematic liquid crystals modeled by a self-consistent molecular field theory, *Phys. Rev. E* **102**, 010701(R) (2020).
- [27] C. D. Parmee, M. R. Dennis, and J. Ruostekoski, Optical excitations of Skyrmions, knotted solitons, and defects in atoms, *Commun. Phys.* **5**, 54 (2022).
- [28] G. Poy, A. J. Hess, A. J. Seracuse, M. Paul, S. Žumer, and I. I. Smalyukh, Interaction and co-assembly of optical and topological solitons, *Nat. Photonics* **16**, 454 (2022).
- [29] S.-Z. Lin and S. Hayami, Ginzburg-Landau theory for skyrmions in inversion-symmetric magnets with competing interactions, *Phys. Rev. B* **93**, 064430 (2016).
- [30] C. Psaroudaki, S. Hoffman, J. Klinovaja, and D. Loss, Quantum Dynamics of Skyrmions in Chiral Magnets, *Phys. Rev. X* **7**, 041045 (2017).
- [31] S. A. Díaz, J. Klinovaja, and D. Loss, Topological Magnons and Edge States in Antiferromagnetic Skyrmion Crystals, *Phys. Rev. Lett.* **122**, 187203 (2019).
- [32] S. A. Díaz, T. Hirokawa, J. Klinovaja, and D. Loss, Chiral magnonic edge states in ferromagnetic skyrmion crystals controlled by magnetic fields, *Phys. Rev. Res.* **2**, 013231 (2020).

- [33] C. Psaroudaki and C. Panagopoulos, Skyrmion Qubits: A New Class of Quantum Logic Elements Based on Nanoscale Magnetization, *Phys. Rev. Lett.* **127**, 067201 (2021).
- [34] S. Hayami, T. Okubo, and Y. Motome, Phase shift in skyrmion crystals, *Nat. Commun.* **12**, 6927 (2021).
- [35] C. Psaroudaki and C. Panagopoulos, Skyrmion helicity: Quantization and quantum tunneling effects, *Phys. Rev. B* **106**, 104422 (2022).
- [36] C. Naya, D. Schubring, M. Shifman, and Z. Wang, Skyrmions and hopfions in three-dimensional frustrated magnets, *Phys. Rev. B* **106**, 094434 (2022).
- [37] S. Hayami, Ferroaxial moment induced by vortex spin texture, *Phys. Rev. B* **106**, 144402 (2022).
- [38] C. Back, V. Cros, H. Ebert, K. Everschor-Sitte, A. Fert, M. Garst, T. Ma, S. Mankovsky, T. L. Monchesky, M. Mostovoy, N. Nagaosa, S. S. P. Parkin, C. Pfeleiderer, N. Reyren, A. Rosch, Y. Taguchi, Y. Tokura, K. von Bergmann, and J. Zang, The 2020 skyrmionics roadmap, *J. Phys. D: Appl. Phys.* **53**, 363001 (2020).
- [39] T. H. R. Skyrme, A non-linear field theory, *Proc. R. Soc. A* **260**, 127 (1961).
- [40] T. H. R. Skyrme, A unified field theory of mesons and baryons, *Nucl. Phys.* **31**, 556 (1962).
- [41] E. Witten, Global aspects of current algebra, *Nucl. Phys. B* **223**, 422 (1983).
- [42] E. Witten, Current algebra, baryons, and quark confinement, *Nucl. Phys. B* **223**, 433 (1983).
- [43] M. Nitta, Matryoshka skyrmions, *Nucl. Phys. B* **872**, 62 (2013).
- [44] L. Šmejkal, Y. Mokrousov, B. Yan, and A. H. MacDonald, Topological antiferromagnetic spintronics, *Nat. Phys.* **14**, 242 (2018).
- [45] V. P. Kravchuk, O. Gomonay, D. D. Sheka, D. R. Rodrigues, K. Everschor-Sitte, J. Sinova, J. van den Brink, and Y. Gaididei, Spin eigenexcitations of an antiferromagnetic skyrmion, *Phys. Rev. B* **99**, 184429 (2019).
- [46] M. Hongo, T. Fujimori, T. Misumi, M. Nitta, and N. Sakai, Instantons in chiral magnets, *Phys. Rev. B* **101**, 104417 (2020).
- [47] B. Göbel, I. Mertig, and O. A. Tretiakov, Beyond skyrmions: Review and perspectives of alternative magnetic quasiparticles, *Phys. Rep.* **895**, 1 (2021).
- [48] A. Qaiumzadeh, L. A. Kristiansen, and A. Brataas, Controlling chiral domain walls in antiferromagnets using spin-wave helicity, *Phys. Rev. B* **97**, 020402(R) (2018).
- [49] M. Nitta, Correspondence between Skyrmions in 2 + 1 and 3 + 1 dimensions, *Phys. Rev. D* **87**, 025013 (2013).
- [50] H. Xia, C. Jin, C. Song, J. Wang, J. Wang, and Q. Liu, Control and manipulation of antiferromagnetic skyrmions in racetrack, *J. Phys. D: Appl. Phys.* **50**, 505005 (2017).
- [51] M. Hoffmann, G. P. Müller, C. Melcher, and S. Blügel, Skyrmion-antiskyrmion racetrack memory in rank-one DMI materials, *Front. Phys.* **9**, 769873 (2021).
- [52] S. S. P. Parkin, M. Hayashi, and L. Thomas, Magnetic domain-wall racetrack memory, *Science* **320**, 190 (2008).
- [53] H. Yu, J. Xiao, and H. Schultheiss, Magnetic texture based magnonics, *Phys. Rep.* **905**, 1 (2021).
- [54] C. Schütte and M. Garst, Magnon-skyrmion scattering in chiral magnets, *Phys. Rev. B* **90**, 094423 (2014).
- [55] S. Schroeter and M. Garst, Scattering of high-energy magnons off a magnetic skyrmion, *Low Temp. Phys.* **41**, 817 (2015).
- [56] K. Y. Guslienko, Gauge and emergent electromagnetic fields for moving magnetic topological solitons, *Europhys. Lett.* **113**, 67002 (2016).
- [57] G. Tatara, Effective gauge field theory of spintronics, *Phys. E* **106**, 208 (2019).
- [58] R. Cheng and Q. Niu, Electron dynamics in slowly varying antiferromagnetic texture, *Phys. Rev. B* **86**, 245118 (2012).
- [59] K. A. van Hoogdalem, Y. Tserkovnyak, and D. Loss, Magnetic texture-induced thermal Hall effects, *Phys. Rev. B* **87**, 024402 (2013).
- [60] B. Li and A. A. Kovalev, Spin superfluidity in noncollinear antiferromagnets, *Phys. Rev. B* **103**, L060406 (2021).
- [61] S. Lee and S. K. Kim, Orbital angular momentum and current-induced motion of a topologically textured domain wall in a ferromagnetic nanotube, *Phys. Rev. B* **104**, L140401 (2021).
- [62] S. Lee and S. K. Kim, Generation of magnon orbital angular momentum by a skyrmion-textured domain wall in a ferromagnetic nanotube, *Front. Phys.* **10**, 858614 (2022).
- [63] P. Yan, X. S. Wang, and X. R. Wang, All-Magnonic Spin-Transfer Torque and Domain Wall Propagation, *Phys. Rev. Lett.* **107**, 177207 (2011).
- [64] S. K. Kim, Y. Tserkovnyak, and O. Tchernyshyov, Propulsion of a domain wall in an antiferromagnet by magnons, *Phys. Rev. B* **90**, 104406 (2014).
- [65] C. V. Sukumar, Supersymmetric quantum mechanics of one-dimensional systems, *J. Phys. A: Math. Gen.* **18**, 2917 (1985).
- [66] F. Cooper, A. Khare, and U. Sukhatme, Supersymmetry and quantum mechanics, *Phys. Rep.* **251**, 267 (1995).
- [67] S. Takei and Y. Tserkovnyak, Superfluid Spin Transport Through Easy-Plane Ferromagnetic Insulators, *Phys. Rev. Lett.* **112**, 227201 (2014).
- [68] S. Takei, B. I. Halperin, A. Yacoby, and Y. Tserkovnyak, Superfluid spin transport through antiferromagnetic insulators, *Phys. Rev. B* **90**, 094408 (2014).
- [69] S. K. Kim and Y. Tserkovnyak, Magnetic Domain Walls as Hosts of Spin Superfluids and Generators of Skyrmions, *Phys. Rev. Lett.* **119**, 047202 (2017).
- [70] S. K. Kim, S. Takei, and Y. Tserkovnyak, Thermally activated phase slips in superfluid spin transport in magnetic wires, *Phys. Rev. B* **93**, 020402(R) (2016).
- [71] G. Go, S. Lee, and S. K. Kim, Generation of nonreciprocity in gapless spin waves by chirality injection, *Phys. Rev. B* **105**, 134401 (2022).
- [72] D. Tchraikian and K. Arthur, Solitons in gauged Sigma models: 2 dimensions, *Phys. Lett. B* **352**, 327 (1995).
- [73] B. Schroers, Gauged sigma models and magnetic Skyrmions, *SciPost Phys.* **7**, 030 (2019).
- [74] M. Speight and T. Winyard, Skyrmions and spin waves in frustrated ferromagnets at low applied magnetic field, *Phys. Rev. B* **101**, 134420 (2020).
- [75] M. Scaglioni, M. Jouanne, M. Balkanski, G. Ouvrard, and G. Benedek, Raman scattering in antiferromagnetic FePS<sub>3</sub> and FePSe<sub>3</sub> crystals, *Phys. Rev. B* **35**, 7097 (1987).
- [76] J.-U. Lee, S. Lee, J. H. Ryoo, S. Kang, T. Y. Kim, P. Kim, C.-H. Park, J.-G. Park, and H. Cheong, Ising-type magnetic ordering in atomically thin FePS<sub>3</sub>, *Nano Lett.* **16**, 7433 (2016).

- [77] K. S. Burch, D. Mandrus, and J.-G. Park, Magnetism in two-dimensional van der Waals materials, *Nature (London)* **563**, 47 (2018).
- [78] T. M. J. Cham, S. Karimeddy, A. H. Dismukes, X. Roy, D. C. Ralph, and Y. K. Luo, Anisotropic gigahertz antiferromagnetic resonances of the easy-axis van der Waals antiferromagnet CrSBr, *Nano Lett.* **22**, 6716 (2022).
- [79] G. G. Ivanov, Symmetries, conservation laws, and exact solutions in nonlinear sigma models, *Theor. Math. Phys.* **57**, 981 (1983).
- [80] F. D. M. Haldane, Nonlinear Field Theory of Large-Spin Heisenberg Antiferromagnets: Semiclassically Quantized Solitons of the One-Dimensional Easy-Axis Néel State, *Phys. Rev. Lett.* **50**, 1153 (1983).
- [81] F. D. M. Haldane, Continuum dynamics of the 1-D Heisenberg antiferromagnet: Identification with the O(3) nonlinear sigma model, *Phys. Lett. A* **93**, 464 (1983).
- [82] N. Hasselmann and P. Kopietz, Spin-wave interactions in quantum antiferromagnets, *Europhys. Lett.* **74**, 1067 (2006).
- [83] M. Kobayashi and M. Nitta, Sine-Gordon kinks on a domain wall ring, *Phys. Rev. D* **87**, 085003 (2013).
- [84] C. Ross and M. Nitta, Domain-wall skyrmions in chiral magnets, *Phys. Rev. B* **107**, 024422 (2023).
- [85] G. H. Derrick, Comments on nonlinear wave equations as models for elementary particles, *J. Math. Phys.* **5**, 1252 (1964).
- [86] S. K. Kim and Y. Tserkovnyak, Chiral Edge Mode in the Coupled Dynamics of Magnetic Solitons in a Honeycomb Lattice, *Phys. Rev. Lett.* **119**, 077204 (2017).
- [87] B. Flebus, H. Ochoa, P. Upadhyaya, and Y. Tserkovnyak, Proposal for dynamic imaging of antiferromagnetic domain wall via quantum-impurity relaxometry, *Phys. Rev. B* **98**, 180409(R) (2018).
- [88] B. Flebus and Y. Tserkovnyak, Entangling distant spin qubits via a magnetic domain wall, *Phys. Rev. B* **99**, 140403(R) (2019).
- [89] B. Li and A. A. Kovalev, Magnon Landau Levels and Spin Responses in Antiferromagnets, *Phys. Rev. Lett.* **125**, 257201 (2020).
- [90] N. Rosen and P. M. Morse, On the vibrations of polyatomic molecules, *Phys. Rev.* **42**, 210 (1932).
- [91] G. Pöschl and E. Teller, Bemerkungen zur Quantenmechanik des anharmonischen Oszillators, *Z. Phys.* **83**, 143 (1933).
- [92] J. Lekner, Reflectionless eigenstates of the  $\text{sech}^2$  potential, *Am. J. Phys.* **75**, 1151 (2007).
- [93] B. Zhang, Z. Wang, Y. Cao, P. Yan, and X. R. Wang, Eavesdropping on spin waves inside the domain-wall nanochannel via three-magnon processes, *Phys. Rev. B* **97**, 094421 (2018).
- [94] M. Gadella, Ş. Kuru, and J. Negro, The hyperbolic step potential: Anti-bound states, SUSY partners and Wigner time delays, *Ann. Phys. (NY)* **379**, 86 (2017).
- [95] P. Boonserm and M. Visser, Quasi-normal frequencies: Key analytic results, *J. High Energ. Phys.* **03** (2011) 073.
- [96] S. K. Kim, K. Nakata, D. Loss, and Y. Tserkovnyak, Tunable Magnonic Thermal Hall Effect in Skyrmion Crystal Phases of Ferrimagnets, *Phys. Rev. Lett.* **122**, 057204 (2019).
- [97] H. Urakawa, *Calculus of Variations and Harmonic Maps* (American Mathematical Society, Providence, 1993).
- [98] M. Fecko, *Differential Geometry and Lie Groups for Physicists* (Cambridge University, Cambridge, England, 2006).
- [99] P. Shen, Y. Tserkovnyak, and S. K. Kim, Driving a magnetized domain wall in an antiferromagnet by magnons, *J. Appl. Phys.* **127**, 223905 (2020).
- [100] P. Yan and G. E. W. Bauer, Magnonic Domain Wall Heat Conductance in Ferromagnetic Wires, *Phys. Rev. Lett.* **109**, 087202 (2012).
- [101] J. P. Pekola and B. Karimi, *Colloquium: Quantum heat transport in condensed matter systems*, *Rev. Mod. Phys.* **93**, 041001 (2021).
- [102] D. Hill, V. Slastikov, and O. Tchernyshyov, Chiral magnetism: A geometric perspective, *SciPost Phys.* **10**, 078 (2021).